AIAA 80-1063R

Acoustic Characteristics of the External Upper Surface Blowing Propulsive-Lift Configuration

Masataka Maita* and Tadao Torisaki†
National Aerospace Laboratory, Tokyo, Japan

Acoustic characteristics of the external upper surface blowing (USB) concept of a propulsive-lift configuration were studied with a full-scale model static experiment. Test components included a FJR710 turbofan engine with an acoustically treated nacelle and a USB wing/flap assembly. These were utilized in conjunction with ground verification testing of the propulsive systems of the National Aerospace Laboratory's Quiet STOL Research Aircraft. Results were compared with the previous 8% scale cold-flow model data. The effect of shielding provided by the wing/flap surface on aft-radiated turbofan engine noise was also studied and some attempts were made to reduce USB noise.

Introduction

EXTERNAL upper surface blowing (USB) is one of the primary concepts for achieving powered high lift in short takeoff and landing (STOL) aircraft. The powered-lift augmentation during takeoff and landing is derived by deflecting the turbofan engine exhaust jet adjacent to the wing/flap upper surface by the Coanda effect.

Short-haul transports employing this design concept will be able to operate from short runways with highly maneuverable, steep, and curved flight paths and to shield some of the aft-radiated turbofan engine noise, which will result in reduced community noise exposure. However, the external upper surface blown flap produces additional noise as the engine exhaust flow interacts with the wing/flap surface. Moreover, this engine noise will be potentially greater because higher power settings may be required during STOL operations.

In order to meet the stringent noise standards now being issued and to obtain community acceptance, noise reduction techniques must be developed. While the state-of-the-art on these subjects is advancing, the details of the actual noise generation and radiation mechanisms are not yet known.

The research program has been undertaken to study the acoustic characteristics of the USB propulsive-lift configuration using the FJR710 turbofan engine and full-scale USB wing/flap assembly model of the NAL Quiet STOL Research Aircraft. The acoustic tests were part of a technology integration program to accomplish initial full-scale engine ground verification testing and to measure the aeroacoustic and thermal wing/flap load environment in order to assess the acoustic fatigue failure of structural members and propulsive-lift performance. The acoustic content included the noise directivity pattern, noise spectra for various USB flap configurations and engine power rates, coherence data between the fluctuating surface pressure and the farfield noise, noise dependence on engine exhaust jet velocity, the engine noise shielding effect of the wing/flap surface, and a determination of the effect of engine exhaust flow attachment devices on noise generation.

In the present paper, we attempt to summarize the principal results and conclusions of USB acoustic characteristics and present a preliminary analysis of the 8% scale cold-flow static model test and some of the noise reduction techniques.

Presented as Paper 80-1063 at the AIAA Aeroacoustics Conference, Hartford, Conn., June 4-6, 1980; submitted July 24, 1980; revision received Jan. 27, 1981.

*Research Official, Noise and Emission Division. Member AIAA.
†Division Head, Noise and Emission Division.

Apparatus and Procedure

The typical setup of the external upper surface blowing propulsive-lift configuration is shown in Fig. 1. The model was powered by a FJR710 turbofan engine which had a bypass ratio of 6.5, rated at approximately 5000 kg static thrust. An acoustic nacelle inlet equipped with a bell mouth was installed in the fan inlet. The FJR710[1] engine was equipped with an $AR_e = 2.66$ (aspect ratio is defined as the nozzle exit area divided by the square of the nozzle maximum height) D nozzle directed downward toward the top of the main wing. The D nozzle kickdown angle was 22 deg. The wing had double flaps and for landing flap configuration ($\delta_f = 60$ deg), apparatus for enhancing the Coanda attachment were employed to prevent the engine exhaust flow separating from the USB flaps. The present USB propulsive-lift configuration simulated the outboard engine propulsive content of NAL Quiet STOL Research Aircraft (cf. Fig. 2). A sketch of the geometry of the engine/wing/flap assembly is presented in Fig. 3. The tests were conducted at the NAL Kakuda branch outdoor test facilities.

The main test parameter variations related to the acoustic measurements were:

1) Engine power setting.

2) USB flap deployment angles, $\delta_f = 0$, 30, and 60 deg representing cruise, takeoff, and landing flap configurations, respectively.

3) Position of engine exhaust flow attachment devices on wing/flaps.

Farfield noise data were taken for all parameter variations by ½ in. B&K condenser microphones placed on a 25 m radius centered at the intersection of the exhaust nozzle plane with the exhaust nozzle centerline, which was 2.5 m above the ground. The microphones were elevated on poles to be in the same horizontal plane as the engine centerline. The surface fluctuating pressures were measured by ¼ in. B&K microphones which were flush mounted on the wing/flaps upper

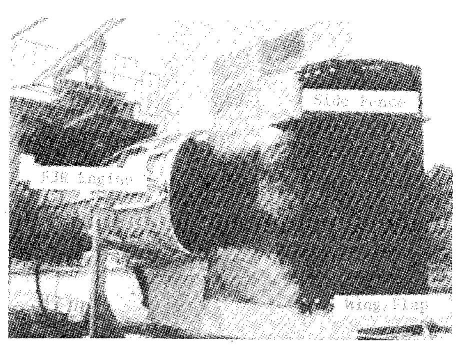

Fig. 1 USB test configuration with side fence installed.

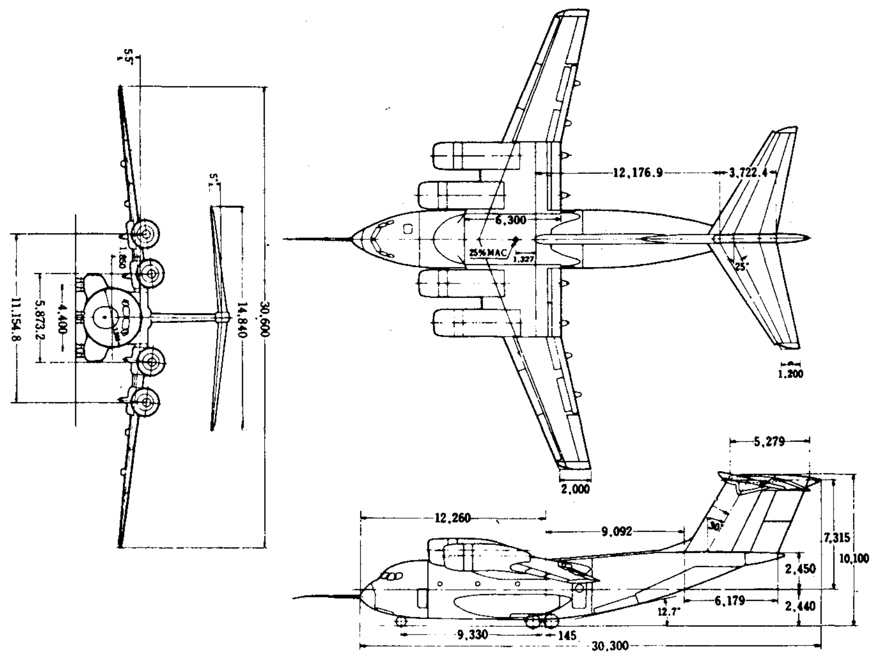

Fig. 2 NAL Quiet STOL Research Aircraft.

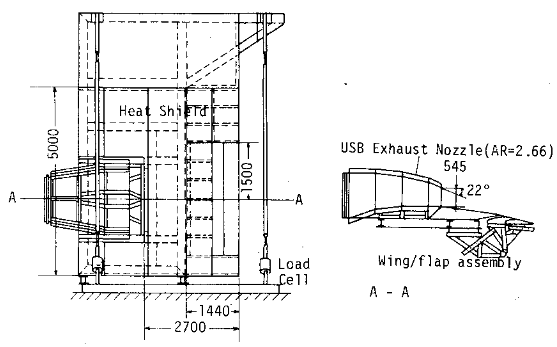

Fig. 3 Geometry of engine-wing/flap assembly.

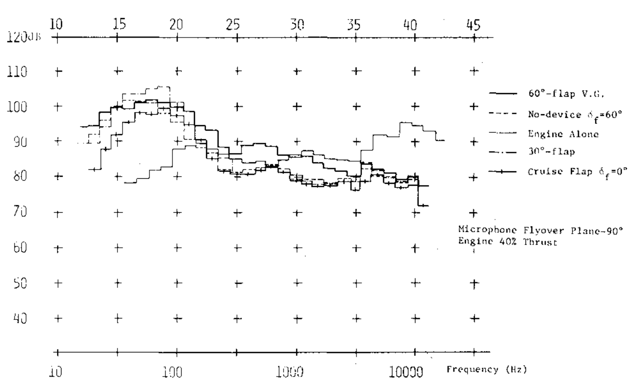

Fig. 4 One-third octave band spectra at flyover – 90 deg direction.

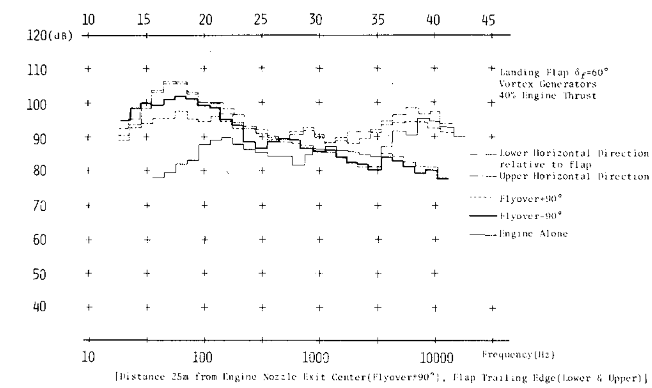

Fig. 5 Comparison of spectra at upper and lower directions for landing flap configuration.

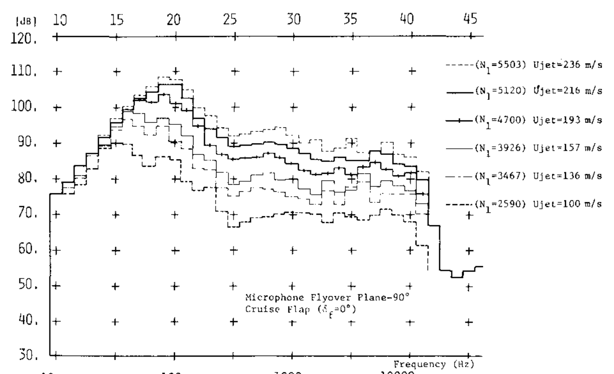

Fig. 6 Effect of exhaust velocity variations on noise spectra.

surface with Teflon-coated adaptors which insured a flat frequency response within ±0.5 dB to 10 kHz over the temperature range up to 150°C.[2] Noise data were FM recorded on a data recorder. No corrections were applied to compensate for the ground reflection interference in the data.

In addition to the acoustic measurement, extensive instrumentations of the engine and other USB environment components were incorporated, which provided for lift force, wing surface static pressures, and surface temperatures, together with engine performance.

Results and Discussion

Presented in Fig. 4 are one-third octave band SPL spectra of cruise, takeoff, and landing USB flap configurations for the case of 40% engine power setting at the microphone position in the flyover plane –90 deg corresponding to directly beneath the wing. These data are compared with the spectrum of the FJR engine alone as the baseline. The high-frequency (above 2000 Hz) noise, predominate in the engine-alone case, are contributed mainly by fan-generated noise. Jet exhaust noise for FJR engine alone has been estimated to have a peak frequency around 160 Hz and is not predominant in this case. The additions of the USB wing/flap system result in a noise increase in the lower frequencies of the spectrum, while in the high-frequency ranges SPL is decreased by the shielding effect of wing/flap surface. (See Fig. 5.) The low-frequency activities (around 100 Hz) in the spectra of USB

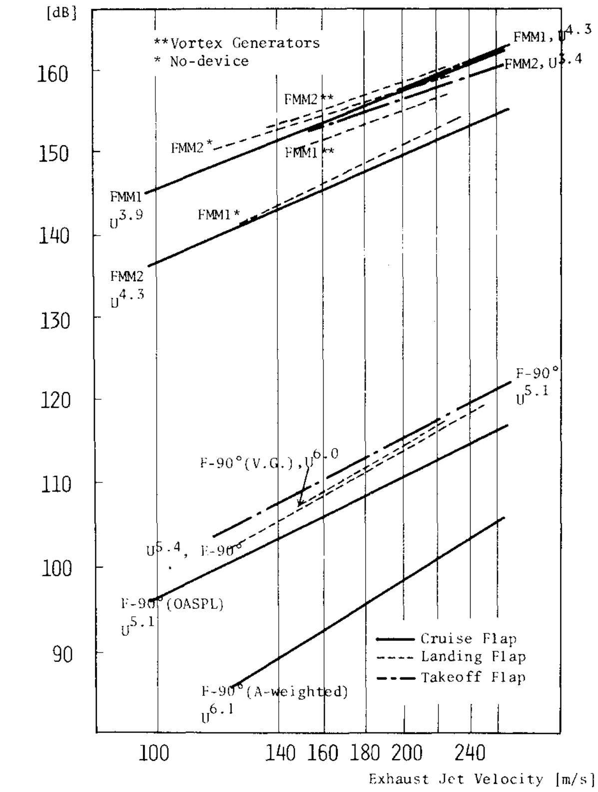

Fig. 7 OASPL dependence on exhaust velocity.

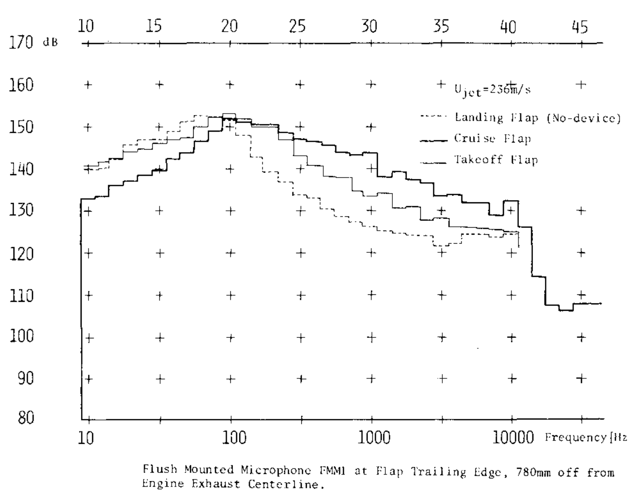

Fig. 8 Fluctuating surface pressure at flap trailing edge.

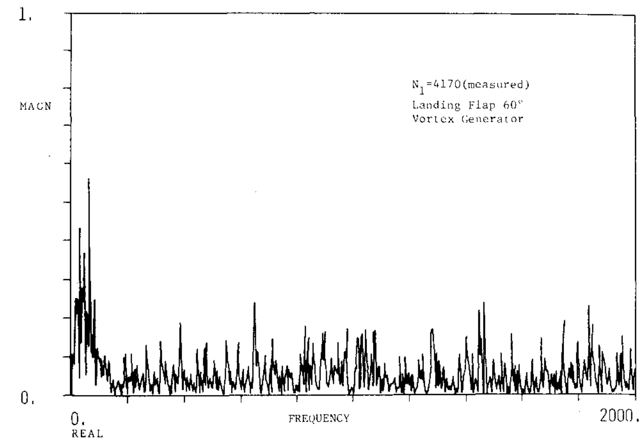

Fig. 9 Coherence between flap trailing edge and flyover – 90 deg.

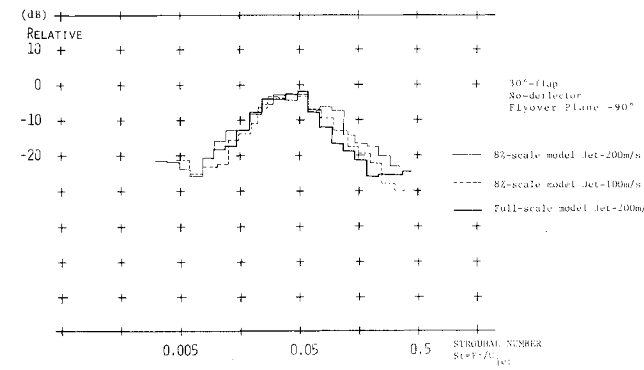

Fig. 10 Normalized SPL spectral density.

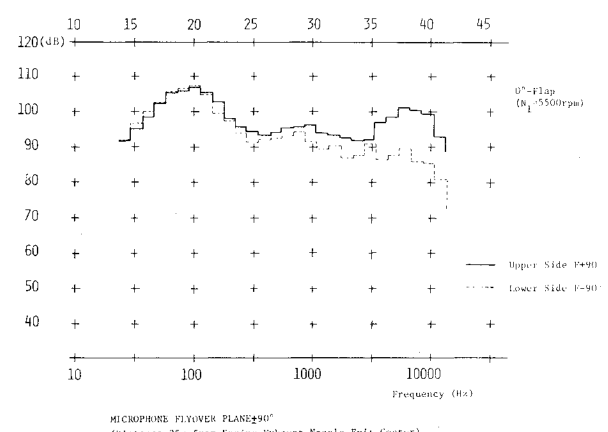

Fig. 11 Comparison of noise spectra at directions below and above the wing.

system noise are the principal contribution of exhaust jet/wing/flap surface interactions as predicted by previous 8% scale cold-flow USB noise studies.[3-5]

The effect of exhaust jet velocity variation on the USB system noise SPL is presented in Fig. 6 for the cruise flap configuration at the −90 deg flyover microphone position. The peak SPL frequency f_{peak} changes correspond approximately to a constant Strouhal number. Overall sound pressure level (OASPL) from the USB configuration varies with exhaust jet velocity according to approximately fifth power law dependence at flyover −90 deg direction as shown by the typical data in Fig. 7. One-third octave band spectra of fluctuating pressure at the flush-mounted microphone FMM1 on the flap trailing edge, 780 mm from engine exhaust centerline, is shown in Fig. 8.

A series of coherence data between fluctuating surface pressure and farfield noise at flyover −90 deg direction were taken. The frequency range of peak coherence was found to be the same as in the farfield noise spectrum when they were taken at the flap trailing edge. Also, for these frequency ranges, the flap trailing edge was the location of the highest magnitude of coherence (see Fig. 9 for an example). Figure 10 shows the normalized SPL spectral density using a Strouhal number based upon the wall jet thickness δ at the flap trailing edge (δ was estimated by comparing experimental data from Reddy et al.,[6] Brown,[7] and others' and approximately 30% of USB nozzle exit height). The Strouhal number corresponding to each spectral peak frequency range is approximately constant at 0.05 for both the 8% scale cold-flow model and the full-scale propulsive system. Normalized SPL densities have similarity in form in the peak level Strouhal number range and scatter outside this range. As predicted by previous 8% scale cold-flow noise studies, the low-frequency activity in the spectra resulted from jet flap/trailing-edge interaction noise.

The preceding results imply that edge noise is essentially independent of jet upstream sources (i.e., whether compressed

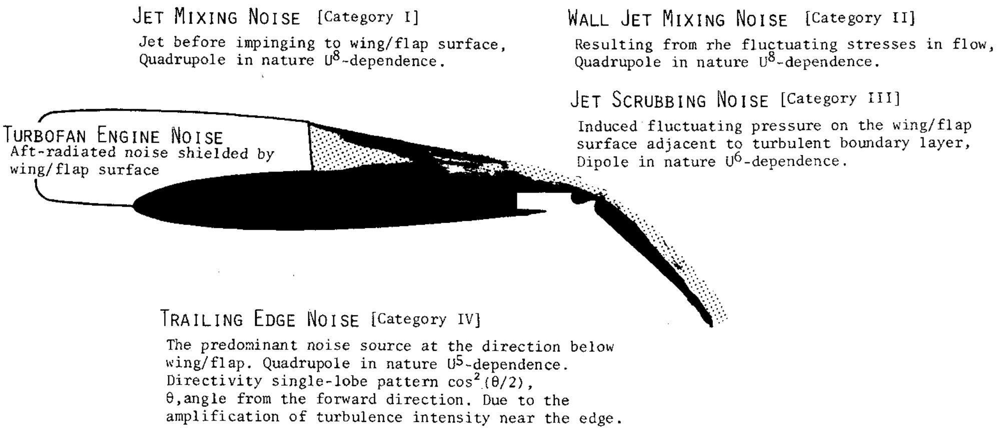

Fig. 12 USB noise categories.

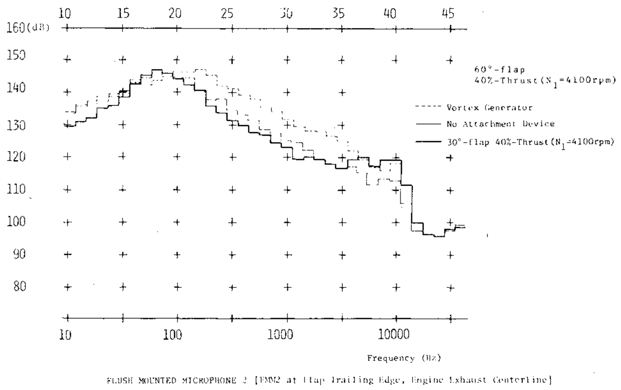

Fig. 13 Effect of vortex generators.

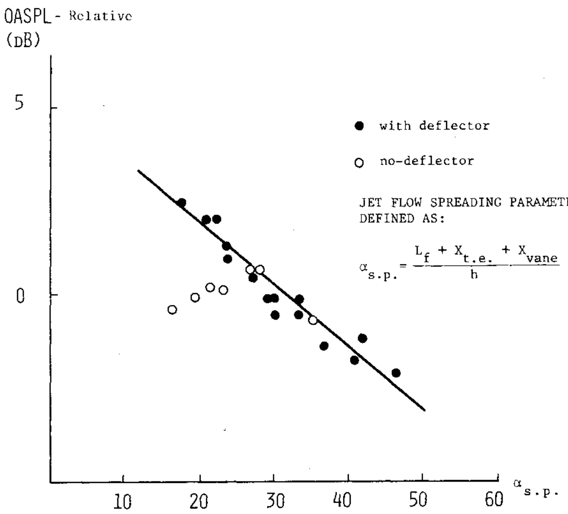

Fig. 14 Noise dependence on $\alpha_{s.p.}$.

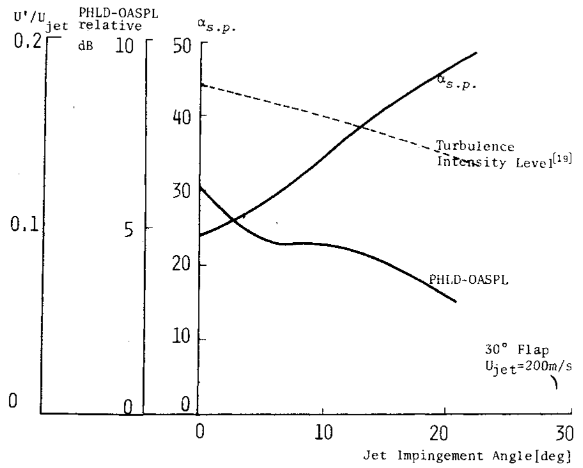

Fig. 15 Effect of jet impingement angle variations on OASPL, $\alpha_{s.p.}$, and turbulence intensity level.

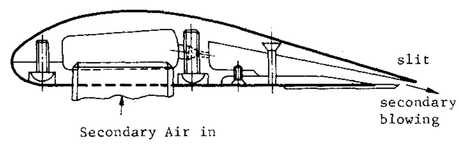

Fig. 16 Slot secondary blowing flap.

air jet or turbofan engine exhaust jet) and Strouhal normalization suggests that the low-frequency noise from actual USB propulsive-lift configurations can be predicted from small-scale cold-flow models. Figure 11 shows a comparison of the noise spectra from the USB system configuration ($\delta_f = 0$ deg) in directions perpendicular to the flap trailing edge below and above the wing/flap (lower and upper parts of the figure, respectively). See Fig. 5 for the $\delta_f = 60$ deg case. In the high-frequency range, the sound levels below the wing are less than the levels above the wing due to the shielding effect by wing/flap surface; however, both peak level frequencies lie in the same band of the low-frequency range with approximately the same SPL intensity. These results are possible since the predominant noise source contributing to the peak SPL frequency ranges is located near the flap trailing edge where the least noise shielding by wing/flap occurs.

From the morphology of past studies, the noise-generating mechanism and its noise source locations on the USB propulsive-lift configuration are organized into the categories summarized in Fig. 12. In the Appendix, theoretical formulations[8-12] which may be applicable to each category are briefly described. (The Ffowcs Williams-Hall arguments employed in the Appendix for the trailing-edge noise-generating mechanism[10] were recently questioned by Tam[13] and Paterson et al.[14] and some modifications would be necessary for certain flowfields where the velocity gradient beneath the jet is very high and highly unstable large-scale flow instabilities are excited.)

Noise radiated from the USB propulsive-lift configuration differs in its fundamental aeroacoustic mechanisms which depend upon its configuration geometries. For the cruise flap configuration ($\delta_f = 0$ deg), as an example, the surface dipole noise is thought to be negligible since, as Phillips[15] or Kraichnan et al.[12] have argued for a plane surface, the strength of surface dipole is equal to the fluctuating viscous stress and hence inviscid flow produces no dipole sound and the plane acts merely to reflect the volume quadrupole. These arguments were extended by Meecham[16] to more general cases where the ratio of wall jet thickness to flap radius of

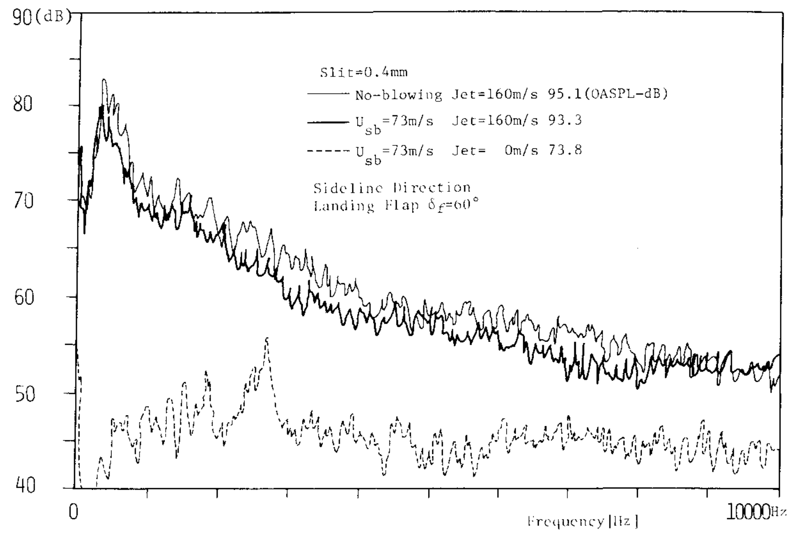

Fig. 17 Noise reduction by slot secondary blowing flap.

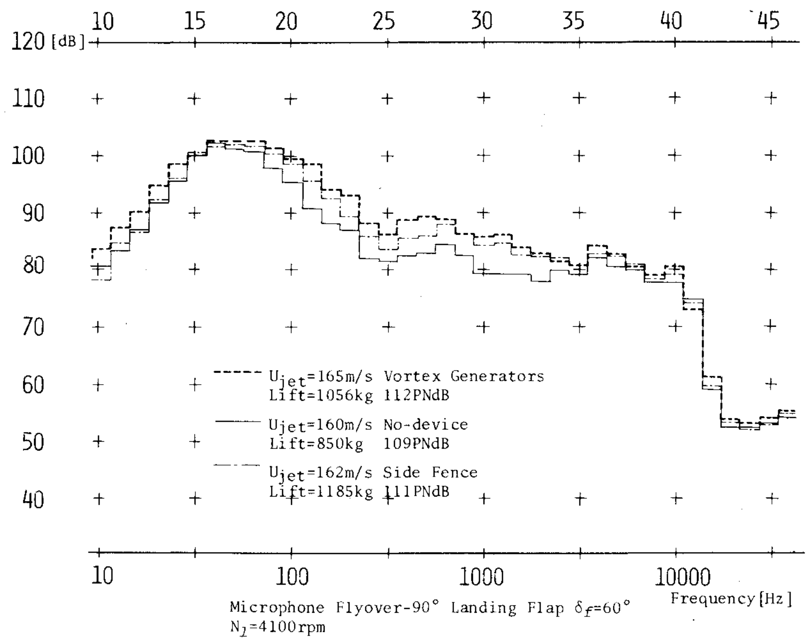

Fig. 18 Effect of side fence.

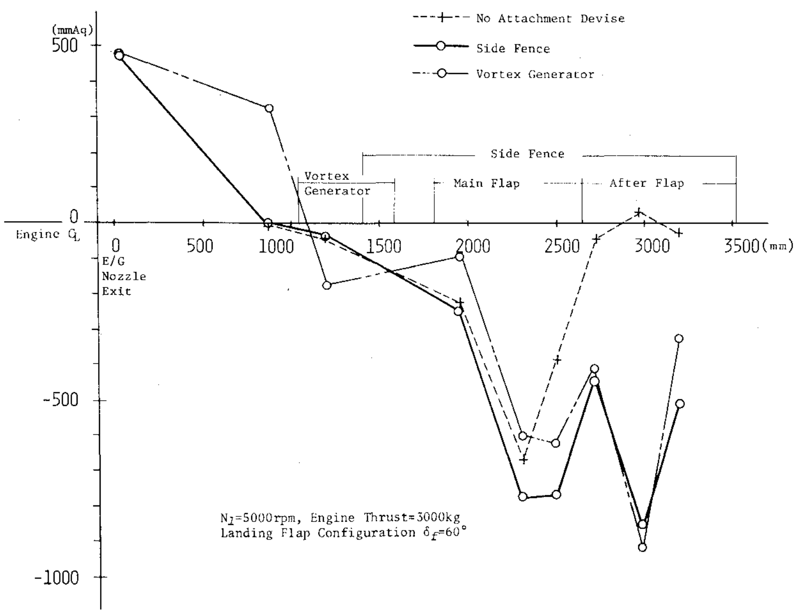

Fig. 19 Static pressure profiles on wing/flap surface along engine centerline.

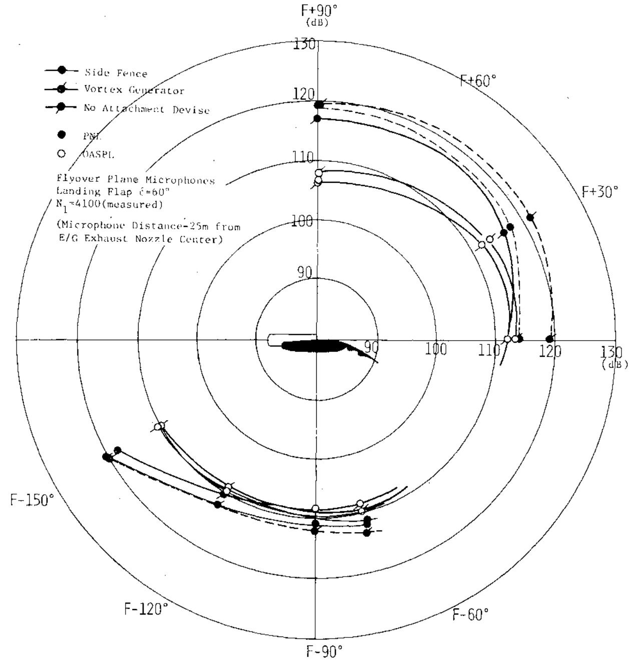

Fig. 20 Directivity patterns of farfield noise.

curvature is of small order. When the vortex generators were installed on wing surface in order to enhance the engine exhaust flow attachment for the landing flap configuration ($\delta_f = 60$ deg), the associated jet vortex rollup phenomenon generates additional noise. One-third octave band spectra at the flap trailing edge (FMM2) for the landing flap configuration with and without vortex generators are presented in Fig. 13. (Compare Figs. 4 and 18 at flyover -90 deg direction.)

In the mid-frequency ranges (around 500 Hz), increases in noise spectral levels were about 6-10 dB. Exhaust velocity on OASPL (at flyover -90 deg direction) was sixth power law dependent and the retraction of vortex generators resulted in lower power law dependence (cf. Fig. 7). However, for the landing flap configuration with no attachment device, the exhaust flow was separated over the aft flap and the exhaust jet/flap edge interaction was different from the configuration with vortex generators. Hence, the noise increases in the spectrum were not solely contributed by the presence of the vortex generators. The jet/edge interaction noise, which is contributive to the spectrum low-frequency activities and the predominant source at the direction below the wing, is dependent on the flowfields near the edge, which also depend upon USB configuration geometries.

In the previous 8% scale experiments, we have attempted to quantify the jet flow spreading and attachment characteristics by introducing the jet flow spreading parameter $\alpha_{s.p.}$ [which was defined as the sum of the attached flow length along the wing/flap surface L_f, the jet spreading spanwise width at fore flap X_{vane} and at after flap trailing edge $X_{t.e.}$ (if totally separated $X_{t.e.} = 0$) divided by the thickness of the jet flow at nozzle exit h] and to compare them with noise data. The dependence of the overall sound pressure level from USB-PHLD (powered high-lift device) measured at the direction below the wing (PHLD-OASPL in abbreviation) on the parameter $\alpha_{s.p.}$ is shown in Fig. 14. The general conclusion obtained is that the better jet flow spreading, the lower PHLD-OASPL for sufficiently attached cases. The qualitative explanation of Fig. 14 is that when jet flow is extensively spread and attached, the turbulence level at the flap trailing edge is eased due to mixing and decay process with thinned wall jet thickness so that the edge noise is weakened and the PHLD-OASPL dominated by edge noise is reduced. The opposite tendency occurs when jet flow is separated on the flap. The jet flow/edge interaction being weak, the PHLD-OASPL is reduced because of reduced edge noise. This process is shown in Fig. 14 for the case with no deflector and parameter $\alpha_{s.p.}$ less than 20. In Fig. 15, the noise, the parameter $\alpha_{s.p.}$, and the turbulence intensity corresponding to various USB nozzle impingement angles are presented.

We have also attempted to attenuate flap edge noise in model experiments by modifying the turbulence flowfield in the vicinity of the trailing edge by slot secondary blowing (cf. Figs. 16 and 17). Controlling edge impedance and either absorbing noise or turbulence energy by treating the flap edge or serrating it are other typical attenuation techniques. Noise reductions by these techniques were not as effective as might be desired, taking into account the structure or performance penalties. The more realistic approach to reduce noise from USB propulsive-lift configurations would be to optimize the USB configuration in such a way that it brought efficient powered lift with cleaner flow deflection. With this in mind, we have been developing the USB propulsive-lift configuration characterized by side fence[16] as the flow attachment device. One-third octave band spectrum (at flyover -90 deg) and lift force attained for the case of USB landing flap configuration with side fence are presented in Fig. 18, compared with the cases of vortex generators and no device. The powered-lift force attained by the side fence-installed USB propulsive configuration system was about 12% higher with a slightly lower noise level, compared with the case of vortex generators.

In Fig. 19, static pressure distributions on wing/flap surface along the engine centerline are presented for the case of 60% engine power setting. Directivity patterns of the farfield noise (in OASPL and perceived noise level) contours for each case are presented in Fig. 20. PNL at the direction below the wing was approximately 8 PNdB lower and 4 PNdB lower than the level at the direction above the wing and the level of engine-alone case, respectively. Spectral differences between the cases of side fence and vortex generators, seen in Fig. 18 (for flyover -90 deg direction) at midfrequencies, are seen in Fig. 20 to have affected differences of approximately 3, 5, and 1 dB in PNL at the directions flyover $+90$, 0, and -90 deg, respectively.

Conclusions

The acoustic characteristics of the external upper surface blowing propulsive-life configuration were studied experimentally using the FJR710 turbofan engine and USB wing/flap assembly. The main conclusions are summarized as follows:

1) Engine exhaust velocity exponents of radiating sound intensity level from USB propulsive-lift configurations varied approximately as U_{jet}^5 at the direction below the wing.

2) Spectral low-frequency noise in the direction below the wing was the principal contribution of jet/flap trailing-edge interaction noise.

3) Normalized SPL spectral densities have similarity in form in the low Strouhal number ranges, which insure the prediction of the low-frequency noise of actual USB propulsive-lift configurations from the small-scale cold-flow model analysis.

4) USB propulsive-lift system with the installation of a side fence was thought to be a promising concept for quiet STOL configurations.

5) Overall fluctuating pressure levels on wing/flap surface exceeded 160 dB for the cases of landing flap configuration at 60% engine power rate and takeoff flap configuration at 90% engine power rate.

6) Some of the aft-radiated turbofan engine noise was shielded by the USB wing/flap. Perceived noise level at the direction below the wing was approximately 4 PNdB lower than the level of turbofan engine alone at 40% engine power rate.

Appendix

Lighthill's Acoustic Analogy

$$\frac{\partial^2 \rho(x,t)}{\partial t^2} - C_0^2 \nabla^2 \rho(x,t) = \frac{\partial^2 T_{ij}}{\partial x_i \partial x_j} \quad [1]$$

$$T_{ij} = \rho u_i u_j + \delta_{ij}(p - C_0^2 \rho) - e_{ij}$$

$$e_{ij} = \mu\left[\frac{\partial u_i}{\partial x_j} + \frac{\partial u_j}{\partial x_i} - \frac{2}{3}\delta_{ij}\frac{\partial u_k}{\partial x_k}\right]$$

Stratton's general solution of the inhomogeneous wave equation [1]

$$\rho - \rho_0 = \frac{1}{4\pi C_0^2}\iiint \frac{\partial^2 T_{ij}}{\partial x_i \partial x_j}\frac{d\chi}{|x-\chi|} + \frac{1}{4\pi}\iint\left[\frac{1}{\xi}\frac{\partial \rho}{\partial n} + \frac{1}{\xi^2}\frac{\partial \xi}{\partial n}\rho + \frac{1}{C_0 \xi}\frac{\partial \xi \partial \rho}{\partial n \partial t}\right] dS(\chi) \quad [2]$$

$\xi = |x - \chi|$

In the absence of solid boundary [2] reduces to the retarded potential solution.

Far-field approximations

$$\rho - \rho_0 = \frac{1}{4\pi C_0^4}\frac{x_i x_j}{x^3}\iiint \frac{\partial^2}{\partial t^2} T_{ij}\left[\chi, t - \frac{\xi}{C_0}\right] d\chi \quad [3]$$

Category I

Curle's Extension

In the absence of solid boundary. Applying Kirchoff's theorem of integration.

$$\rho - \rho_0 = \frac{1}{4\pi C_0^2}\frac{\partial^2}{\partial x_i \partial x_j}\iiint \frac{T_{ij}\left[\chi, t - \frac{\xi}{C_0}\right]}{\xi} d\chi - \frac{1}{4\pi C_0^2}\frac{\partial}{\partial x_i}\iint \frac{-p n_i + n_j e_{ij}}{\xi}\left[\chi, t - \frac{\xi}{C_0}\right] dS(\chi) \quad [4]$$

Second term of [4] Intensity level scales as

$$I_{Scrubbing} \sim \frac{\rho_0 U_{jet}^6}{C_0^3 \gamma^2}\iint \sin^2\Theta\,[\bar{p}^2/q_{jet}^2]\,d\chi \quad [5]$$

integral over scrubbed surface

Boundary condition using Green's function whose normal derivative vanishes on the half-plane. The strength of surface dipole is equal to the fluctuating viscous stress, i.e. vanishes for inviscid flow.

$$\rho - \rho_0 = \frac{1}{4\pi C_0^2}\frac{\partial^2}{\partial x_i \partial x_j}\iiint \frac{\bar{T}_{ij}\left(\chi, t - \frac{\xi}{C_0}\right)}{\xi} d\chi$$

$$\bar{T}_{ij} = T_{ij}(x_I, x_{II}, x_{III}, \tau) \quad \text{if } x_{II} > 0$$
$$= T^*_{ij} = (-1)^{i+j}\, T_{ij}(x_I, -x_{II}, x_{III}, \tau) \quad \text{if } x_{II} < 0$$

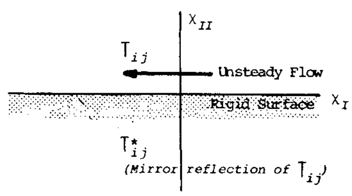

Infinite-plane Surface

McDonald's form of Green's function [Ffowcs-Williams and Hall's formulation]

Scattering Half-plane

$$I_{edge} \sim \frac{\rho_0 U_{jet}^5 T_{int}^4}{C_0^2 r^2}\cos^2\left[\frac{\Theta}{2}\right]\delta_s^2$$

T_{int} *Turbulence Intensity*
δ_c *Correlation Length*
r *Farfield Distance*

Θ, *angle from the forward direction*

Category IV

References

[1] Matsuki, M., "Recent Status on Research and Development of FJR710 Turbofan Engine," ASME Paper S-1, 1977.

[2] B&K Microphone Product Data.

[3] Maita, M. *et.al., Proceedings of 10th Fluid Mechanics Conference*, The Japan Society for Aeronautical and Space Sciences, 1978, pp. 136-143 (in Japanese).

[4] Maita, M. *et.al., Proceedings of 11th Fluid Mechanics Conference*, 1979, pp. 192-199 (in Japanese).

[5] Maita, M., "Jet-Wing/Flap Interaction Noise from USB Configuration," *Theoretical and Applied Mechanics*, Vol. 28, University of Tokyo Press, Tokyo, 1980, pp. 505-521.

[6] Reddy, N. and Brown, W.H., "USB Flow Characteristics Related to Noise Generations," NASA SP-406, 1976.

[7] Brown, H., "USB Flow Properties Related to Noise Generation," Lockheed-Georgia Engineering Rept. LG74R0129, 1974.

[8] Lighthill, M.J., "On Sound Generated Aerodynamically," *Proceedings of the Royal Society,* London, Vol. A211, 1952, pp. 564-587 and Vol. A267, 1962, pp. 147-182.

[9] Curle, N., "The Influence of Solid Boundaries on Aerodynamic Sound," *Proceedings of the Royal Society,* London, Vol. A321, 1955, pp. 505-514.

[10] Ffowcs Williams, J.E. and Hall, L.H., "Aerodynamic Sound Generated by Turbulent Flow in the Vicinity of a Scattering Half Plane," *Journal of Fluid Mechanics*, Vol. 40, 1970, pp. 657-670.

[11] Powell, A., "Aerodynamic Noise and the Plane Boundary," *Journal of the Acoustical Society of America*, Vol. 32, 1960, pp. 982-990.

[12] Kraichnan, R.H., "Pressure Fluctuations in Turbulent Flow over a Flat Plate," *Journal of the Acoustical Society of America*, Vol. 28, 1056, pp. 378-390.

[13] Tam, C.K.W, "Discrete Tones of Isolated Airfoils," *Journal of the Acoustical Society of America*, Vol. 55, 1974, pp. 1173-1177. Also AIAA Paper 75-489, 1975.

[14] Paterson, R.W., Vogt, P.G., and Fink, M.R., "Vortex Noise of Isolated Airfoils," *Journal of Aircraft*, Vol. 10, 1973, pp. 296-302.

[15] Phillips, O.M., "Aerodynamic Sound Radiated from a Turbulent Boundary Layer," *Journal of the Acoustical Society of America*, Vol. 30, 1958, p. 680 (A).

[16] Meechamn, W.C., "Surface and Volume Sound from Boundary Layers," *Journal of the Acoustical Society of America*, Vol. 37, 1965, pp. 516-521.

[17] Maita, M.,Torisaki, T., and Matsuki, M., "Development of the External Upper Surface Blowing Propulsive-Lift Device," AIAA Paper 80-1244, 1980.

[18] Brown, W.H. and Reddy, N.N., "Acoustic Characteristics of an Upper Surface Blowing Concept of Power-Lift System," AIAA Paper 75-204, 1975.